

Many-body effects in the out-of-equilibrium dynamics of a composite bosonic Josephson junction

Sudip Kumar Halder^{a,*}, Anal Bhowmik^{b,c}, Ofir E. Alon^{b,c}

^aDepartment of Physics, SRM University Delhi-NCR Rajiv Gandhi Education city, Sonapat, 131029, India

^bDepartment of Physics, University of Haifa Haifa, 3498838, Israel

^cHaifa Research Center for Theoretical Physics and Astrophysics, University of Haifa Haifa, 3498838, Israel

Abstract

The out-of-equilibrium many-body quantum dynamics of an interacting Bose gas trapped in a one-dimensional composite double-well potential is studied by solving the many-body Schrödinger equation numerically accurately by employing the multiconfigurational time-dependent Hartree for bosons (MCTDHB) method. The composite double-well is formed by merging two deformed harmonic wells having a hump at their centre. We characterised the dynamics by the time evolution of survival probability, fragmentation, and many-particle position and momentum variances. Our study demonstrates the prominent role played by the higher orbitals in the dynamics and thereby highlighted the necessity of a many-body technique like MCTDHB which can take into account all the relevant orbitals for the accurate description of complex many-body dynamics. Further, we showed that the universality of fragmentation with respect to the number of particles corresponding to a particular interaction strength is also exhibited by the higher-order orbitals. Therefore, it is a robust phenomenon not limited to systems that can be described by two orbitals only.

1. Introduction

Ultra-cold atomic systems and quantum gases have emerged as popular tools for the quantum simulation of condensed-matter problems due to their exceptional controllability over the system parameters. Various trapping geometries [1, 2], created utilizing the advanced technique [3, 4, 5, 6], and controlling the underlying inter-particle interactions via Feshbach resonances [7] unveil numerous fundamental and intriguing physical phenomena which were elusive until recently.

Trapping of ultra-cold bosons in a symmetric double-well potential is popularly known as the bosonic Josephson junction (BJJ) [8, 9, 10], which represents a prototype of the Josephson effect initially predicted for tunnelling of Cooper pair between two weakly linked superconductors [11]. Ultra-cold many-body bosons in BJJ provide insight into the tunnelling of correlated quantum dynamics and naturally attract immense interest from the physics community. Examples are fragmentations [12, 13, 14], Josephson oscillations [15], macroscopic self-trapping [16], collapse and revival sequences [17], matter wave interferometry [18], and atomic squeezing state [19, 20], etc..

The BJJ has been extensively studied both theoretically and experimentally [21, 16, 22, 23, 24, 25, 26]. Theoretically, two commonly used methods for the study of BJJ dynamics are the mean-field method and the Bose-Hubbard model. As previously mentioned several features of BJJ dynamics, such as the

collapse and revival of the density oscillations and the fragmentation are beyond the scope of the mean-field level of theory. While the two-mode Bose-Hubbard model can explain those features accurately as long as the dynamics of the BJJ involve only the lowest energy band. Therefore, in order to accurately study the BJJ dynamics when the higher energy bands participate, one requires to solve the full many-body Schrodinger equation. In this context, our group has developed a numerically exact many-body method, called the Multiconfigurational time-dependent Hartree method for bosons (MCTDHB), which takes into account all the participating energy bands, unlike the two-mode Bose-Hubbard model where only the lowest band participates.

In recent times, MCTDHB has been thoroughly used to study the BJJ dynamics in different situations, viz., in 1D as well as in 2D; with repulsive and attractive interactions [27]; with contact and finite range interactions [28, 9, 29]; and in presence of an asymmetry in the trap [30, 31], etc. Fragmentation and the uncertainty product of the many-particle position and momentum operators have also been studied [32] which reasserted the importance of using a full many-body model such as MCDTHB. The many-body uncertainty product of the BEC in a double well was shown to grow with time t as t^2 (up to leading order in t). It has been further shown that, contrary to the BH dimer, the full many-body dynamics of BJJ for the repulsive and attractive interactions are not equivalent [27]. A universality of the degree of fragmentation with respect to different particle numbers N (i.e., fragmentation of the systems to the same value of natural occupations), keeping the interaction parameter $\Lambda = \lambda_0(N - 1)$ fixed (λ_0 being the strength of interaction) has been predicted in the dynamics of interacting bosons in a symmetric as well

*Corresponding Author

Email address: sudip.k@srmuniversity.ac.in (Sudip Kumar Halder)

as an asymmetric double well for the sufficiently strong interaction. Moreover, resonantly enhanced tunnelling which was earlier experimentally observed has also been demonstrated for an asymmetric BJJ with MCTDHB [30]. Moreover, on a different note, the Josephson effects have been investigated in various complex systems, such as, two-component BEC [33], spinor condensates [34], polariton condensates [35], fermionic superfluid [36], and spin-orbit coupled BEC [26].

Although various intriguing many-body effects have already been observed in one-dimensional ultra-cold bosonic ensembles, in all those studies only the lowest band had a significant role in the investigated parameter regime. In order to explore the role of higher energy bands in the many-body dynamics in one spatial dimension, in this work, we propose to study the many-body dynamics of an interacting bosonic system in a composite double well. A composite double well is formed by merging two wells and each of which has a small hump at its centre. To characterise the dynamics, we studied the time evolution of several dynamical quantities such as survival probability, fragmentation, many-particle position and momentum variances, out of which fragmentation and many-particle position and momentum variances are purely many-body quantities. In this work, we showed that an accurate description of the complex many-body dynamics requires a many-body method that takes into account all relevant orbitals. Additionally, we showed that the universality of fragmentation is a global many-body phenomenon.

We organise the paper as follows. Section 2 introduces the system studied here and gives an outline of the methodology used. We discuss our findings in section 3. We summarise our main findings and draw our conclusions in section 4. Further details of the methodology as well as the discussion about the numerical convergence of our results are discussed in Appendix.

2. Theoretical framework

Here we are interested in the dynamics of a system of N interacting structureless bosons in a one-dimensional (1D) potential given by

$$V_{Trap}(x) = V_T(x) + V_0 \exp[-a(x+2)^2] + V_0 \exp[-a(x-2)^2] \quad (1)$$

where

$$V_T(x) = \begin{cases} \frac{1}{2}(x+2)^2, & x < -\frac{1}{2} \\ \frac{3}{2}(1-x^2), & |x| \leq \frac{1}{2} \\ \frac{1}{2}(x-2)^2, & x > \frac{1}{2} \end{cases} \quad (2)$$

We prepare the initial state of the system in the ground state of

$$V_{Trap}(x) = \frac{1}{2}(x+2)^2 + V_0 \exp[-a(x+2)^2] \quad (3)$$

and make it propagate in $V_{Trap}(x)$. The dynamics of this many-body system are governed by the time-dependent many-body Schrödinger equation:

$$\hat{H}\Psi = i \frac{\partial \Psi}{\partial t}, \quad (4)$$

$$\hat{H}(x_1, x_2, \dots, x_N) = \sum_{j=1}^N \hat{h}(x_j) + \sum_{k>j=1}^N W(x_j - x_k).$$

Here x_j is the coordinate of the j -th boson, $\hat{h}(x) = \hat{T}(x) + V_{Trap}(x)$ is the one-body Hamiltonian containing kinetic energy $T(x)$ and a trapping potential $V_{Trap}(x)$ terms, and $W(x_j - x_k)$ is the pairwise interaction between the j -th and k -th bosons. Dimensionless units are employed throughout this work. We used a dimensionless unit in this work.

For our present system, the time-dependent many-boson Schrödinger equation (4) cannot be solved exactly (analytically). Thus, we have deployed an in-principle numerically exact many-body method, MCTDHB, [37, 38] which has been developed by our group and bench-marked with an exactly-solvable model [39, 40]. This method has already been extensively used in the literature [8, 41, 42, 28, 43, 44, 45, 46, 47, 48, 49, 50, 9, 6, 30, 51, 10, 29, 52]. A detailed derivation of the MCTDHB equation of motions can be found in [38, 51]. However, for completeness, we provide a brief description of the method in the Appendix.

3. Result

In this section, we present our findings of the study on the many-body dynamics of an interacting bosonic gas in a composite double well as defined in Eq. (2). Our main purpose of this study is to explore the role of higher energy bands in the many-body dynamics. To understand the characteristics that are exclusively due to the participation of the higher-order energy bands, we will compare our results with the many-body dynamics in a symmetric double well in which only the lowest energy band has a significant role.

3.1. Many-body dynamics

As mentioned earlier, we prepared the initial state in the ground state of the left well [Eq. 3] of the composite double well. Owing to the different values of V_0 , the ground states have acquired complicated shapes. Here it is worth mentioning that due to the symmetry of the trapping potential with respect to reflection, the many-body dynamics are independent of the choice of whether the ground states are prepared in the right-hand side well or the left-hand side well. In this work, we considered a system of $N = 100$ bosons interacting via a contact δ -potential of interaction parameter $\Lambda = 0.1$. In order to understand the participation of the higher-order energy bands in the dynamics, we varied the trap geometry by tuning V_0 while keeping $a = 10$ fixed and bench-marked our findings with the corresponding results of the BJJ. We will characterize the dynamics through the time evolution of several physical quantities such as the survival probability, depletion and fragmentation, and many-particle position and momentum variances.

3.1.1. Survival probability

The survival probability $p_L(t)$, which is a measure of density oscillations between the composite double wells, can be defined as

$$p_L(t) = \int_{-\infty}^0 dx \frac{\rho(x; t)}{N}, \quad (5)$$

where $\rho(x; t)$ is the density in the left composite well. It is closely connected to the population imbalance which is routinely studied in the experiments. In Fig. 1, we plot the survival probability $p_L(t)$ in the left well for different values of V_0 . For $V_0 = 0$, we get back the standard BJJ comprising of two symmetrical wells connected through a barrier and accordingly, $p_L(t)$ also exhibits the usual collapse of density oscillations with time. As V_0 is increased from zero, a hump appears in either well of the BJJ and it turns into the composite BJJ. We observe that irregularity appears in the oscillations of the $p_L(t)$ for $V_0 \neq 0$. Further, the irregularities enhance with the increase in V_0 . With further increase in V_0 , we observe two distinct oscillations for $V_0 = 10$. The high-frequency oscillations indicate the tunnelling between the two adjacent shallow wells whereas the low-frequency oscillations, appearing as the envelope to the high-frequency oscillations, can be attributed to the tunnelling of the whole system between the two composite double wells. The different rates of decay of the density oscillations depending on the values of V_0 come from the initial shape of the ground orbital.

3.1.2. Fragmentation

Fragmentation of BEC provides information about the relative macroscopic populations in higher-order energy levels. The connection between the damping of density oscillations and the fragmentation for a BJJ is already well demonstrated in Ref. [8]. Naturally, our findings for the $p_L(t)$ mentioned above demand a study of the fragmentation as a function of time for various heights of the hump V_0 . This would help us to correlate the changes in density oscillations with the participation of higher-order energy bands.

The development of fragmentation in the system is characterized by the time evolution of the natural occupations per particle $\frac{n_i}{N}$. The system is said to be condensed if $\frac{n_1}{N} \sim \mathcal{O}(1)$. On the other hand, the system is fragmented if $\frac{n_i}{N} \sim \mathcal{O}(1)$ for more than one orbital.

We present our results in Fig. 2. It is found that at $t = 0$, for all the values of V_0 , only the ground orbital is occupied. It signifies that although the shape of the ground state is modified due to different values of V_0 , the coherency of it is unchanged. At $t > 0$, we find that the system gradually becomes fragmented for all V_0 . While for BJJ ($V_0 = 0$) the system becomes two-fold fragmented, the degree of fragmentation increases for $V_0 \neq 0$. For BJJ ($V_0 = 0$), after a sufficiently long time, the system becomes two-fold fragmented with $\frac{n_1}{N} \approx 60\%$ and $\frac{n_2}{N} \approx 40\%$ while the occupations in all higher orbitals are negligibly small. Therefore, a BJJ can be accurately described with only $M = 2$ orbitals. However, the occupations in the third and fourth orbitals start increasing with an increase in V_0 at the cost of occupations in the first and second orbitals. While for $V_0 = 2.5$,

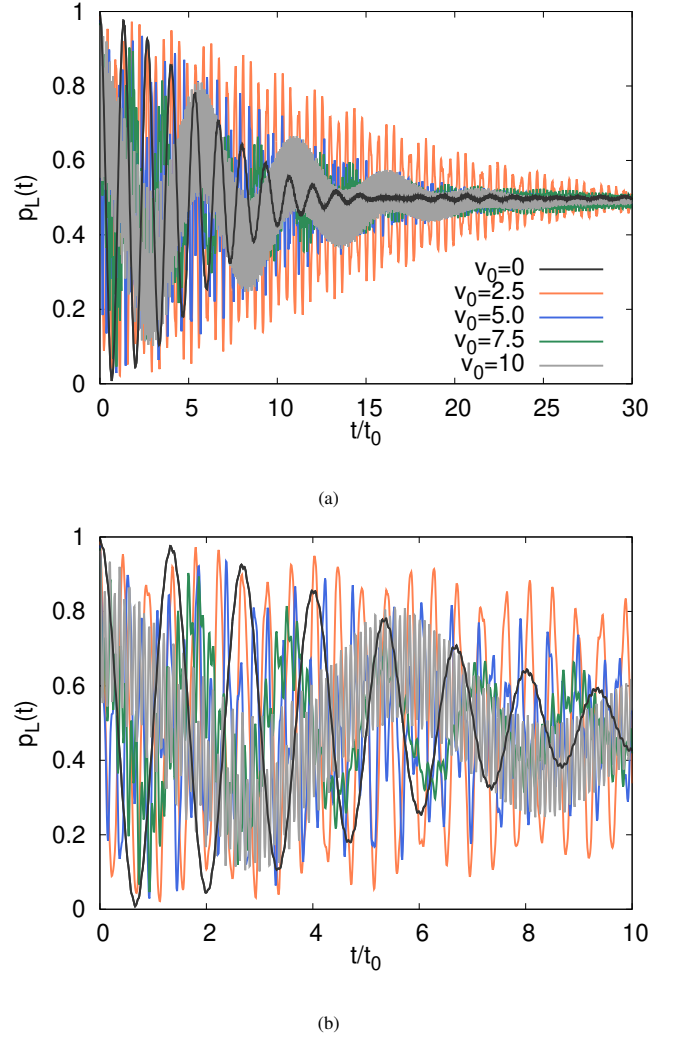


Figure 1: Plot of the $p_L(t)$ as a function of time t for various barrier heights V_0 [panel (a)]. The magnified view of the first few oscillations of $p_L(t)$ is shown in panel (b). Colour codes are explained in panel (a). These results are obtained with $M = 4$ orbitals for $N = 100$ particles with interaction strength $\Lambda = 0.1$.

we see $\frac{n_3}{N} \approx 5\%$, it grows to over $\frac{n_3}{N} \approx 20\%$ for $V_0 = 10$. Similarly, $\frac{n_4}{N}$ which is very small for $V_0 = 2.5$ grows to $\frac{n_4}{N} \approx 5\%$ for $V_0 = 10$. Accordingly, the occupations in the first orbital reduces from $\frac{n_1}{N} \sim 60\%$ for $V_0 = 0$ to $\frac{n_1}{N} \sim 50\%$ for $V_0 = 2.5$, $\frac{n_1}{N} \sim 45\%$ for $V_0 = 5$, $\frac{n_1}{N} \sim 37\%$ for $V_0 = 7.5$. With further increase in V_0 to $V_0 = 10$, there is no significant variation in $\frac{n_1}{N}$. Similarly, $\frac{n_2}{N}$ first increases from $\frac{n_2}{N} \sim 40\%$ for $V_0 = 0$ to $\frac{n_2}{N} \sim 50\%$ for $V_0 = 2.5$, and then gradually decreases to $\frac{n_2}{N} \sim 45\%$ for $V_0 = 5$, $\frac{n_2}{N} \sim 35\%$ for $V_0 = 7.5$, and finally to $\frac{n_2}{N} \sim 32\%$ for $V_0 = 10$. So initially, primarily the second orbital gains population at the cost of the first orbital and both the orbital achieve similar occupations for $V_0 = 2.5$. With further increase in V_0 , particles are transferred to the third and fourth orbitals from the first two orbitals. So, for $V_0 = 5$ the occupations in the first and second orbitals become closer and at the same time occupations in the third and fourth orbitals also increase. While there is a further reduction in occupations in both

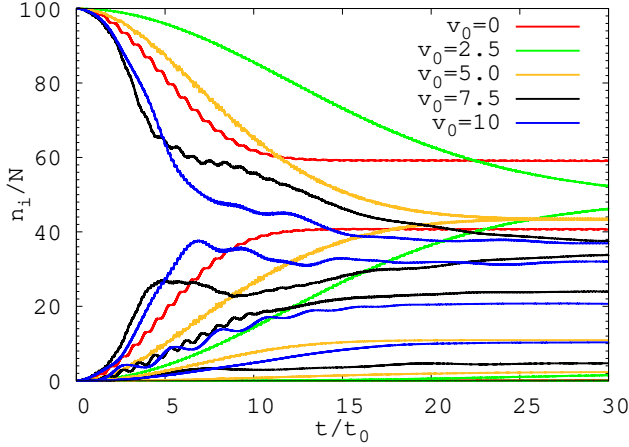


Figure 2: Plot of $\frac{n_i}{N}$ ($i = 1, 2, 3, \text{and } 4$) for BJJ ($V_0 = 0$) and the composite BJJ with various barrier heights V_0 . These results are obtained with $M = 4$ orbitals for a system of $N = 100$ particles with interaction strength $\Lambda = 0.1$.

of the first two orbitals, more particles transfer from the second orbital resulting in reduced occupations in the second orbital. Finally, as V_0 increases to $V_0 = 10$ from $V_0 = 7.5$, there is further redistribution of particles among the second, third and fourth orbitals so that $\frac{n_1}{N}$ remains practically the same. Therefore it is evident that there is a redistribution of the particles among the orbitals and finally, for significantly large V_0 there is a more equitable distribution of the population. This clearly indicates the greater role played by the higher order orbitals in the tunnelling dynamics of the CBJJ ($V_0 \neq 0$).

In this connection, it is instructive to note that the density oscillations die out in BJJ as the system becomes correlated. However, the damping slows down for the CBJJ even though the CBJJ is more fragmented than BJJ. This may be attributed to the delay in the growth of fragmentation in CBJJ for smaller values of V_0 . But for $V_0 \geq 7.5$, the damping is slower even though the correlation in the system grows faster than BJJ. This shows the complicated relationship between the damping of density oscillations and the growth of correlation in the system in the case of CBJJ.

3.1.3. Many-particle position and momentum variances

Next, we consider the many-particle position and momentum variances of the system which is a measure of the quantum resolution of measurement of any observable. Although these cannot be measured easily, these are fundamental quantities due to their connection with the uncertainty principle. Contrary to fragmentation, which reflects only relative occupations, many-body variances are dependent on the actual number of fragmented atoms. Therefore, these are expected to bear more prominent signatures of the actual occupations in higher orbitals and thereby may throw more light on the role of higher-order orbitals in the dynamics.

One can calculate the variance per particle $\frac{1}{N}\Delta_A^2(t)$ for any many-body operator $\hat{A} = \sum_{j=1}^N \hat{a}(x_j)$, which is obtained from single-particle Hermitian operator $\hat{a}(x_j)$, by

$$\begin{aligned} \frac{1}{N}\Delta_A^2(t) &= \frac{1}{N} \left[\langle \Psi(t) | \hat{A}^2 | \Psi(t) \rangle - \langle \Psi(t) | \hat{A} | \Psi(t) \rangle^2 \right] \quad (6) \\ &\equiv \Delta_{\hat{a}, \text{density}}^2(t) + \Delta_{\hat{a}, \text{MB}}^2(t), \\ \Delta_{\hat{a}, \text{density}}^2(t) &= \int dx \frac{\rho(x; t)}{N} a^2(x) - \left[\int dx \frac{\rho(x; t)}{N} a(x) \right]^2, \\ \Delta_{\hat{a}, \text{MB}}^2(t) &= \frac{\rho_{1111}(t)}{N} \left[\int dx |\phi_1^{\text{NO}}(x; t)|^2 a(x) \right]^2 \\ &\quad - (N-1) \left[\int dx \frac{\rho(x; t)}{N} a(x) \right]^2 \\ &\quad + \sum_{jpkq \neq 1111} \frac{\rho_{jpkq}(t)}{N} \left[\int dx \phi_j^{\text{NO}}(x; t) \phi_k^{\text{NO}}(x; t) a(x) \right] \\ &\quad \times \left[\int dx \phi_p^{\text{NO}}(x; t) \phi_q^{\text{NO}}(x; t) a(x) \right]. \end{aligned}$$

Accordingly in Fig. 3 (a), we present our results for the many-particle position variance while Fig. 3 (b) depicts the results for the many-particle momentum variance.

For $V_0 = 0$, we again get back the oscillatory growth of $\frac{1}{N}\Delta_X^2$ with time followed by the saturation as the density oscillation collapses. For $V_0 \neq 0$, we get the overall behaviour quite similar to the BJJ but the main difference lies in the details. For a small value of $V_0 = 2.5$, the growth rate of $\frac{1}{N}\Delta_X^2$ becomes slower which is consistent with the fragmentation dynamics. However, the fluctuations in the saturation value are very high for such a small value of V_0 . With a further increase of V_0 , the growth rate of $\frac{1}{N}\Delta_X^2$ increases but still remains slower than BJJ. Also, the fluctuations reduce drastically for higher values of V_0 .

The fluctuations in $\frac{1}{N}\Delta_X^2$ about the saturation value are the manifestation of the breathing oscillations within the two wells of each of the compound wells. For small intra-well barrier height V_0 , large breathing oscillations between the two wells of each compound wells lead to large fluctuations in $\frac{1}{N}\Delta_X^2$. With increasing V_0 , the breathing oscillations get damped leading to smaller fluctuations in $\frac{1}{N}\Delta_X^2$ for higher values of V_0 .

The dynamics of atoms will have a more prominent impact on the many-particle momentum variance. Naturally, we again observe fluctuations in $\frac{1}{N}\Delta_{\hat{p}_x}^2$ around a mean value for BJJ ($V_0 = 0$). For a small V_0 , we observe very large fluctuations in $\frac{1}{N}\Delta_{\hat{p}_x}^2$ due to the large breathing oscillations. With further increase in V_0 , the damping in the intra-well breathing oscillations results in the gradual reduction in fluctuations of $\frac{1}{N}\Delta_{\hat{p}_x}^2$. For such values of V_0 , $\frac{1}{N}\Delta_{\hat{p}_x}^2$ fluctuates around a mean value which initially increases slightly with time before stabilising to a saturation value. This saturation value also depends on V_0 and first increases before gradually decreasing with increasing V_0 .

3.2. Universality of fragmentation

Since the participation of the higher-order energy bands significantly affected the growth of fragmentation in the system, it is natural to ask about its impact on the universality of the degree of fragmentation with respect to N . It is a novel phenomenon predicted for the BJJ dynamics when only a single

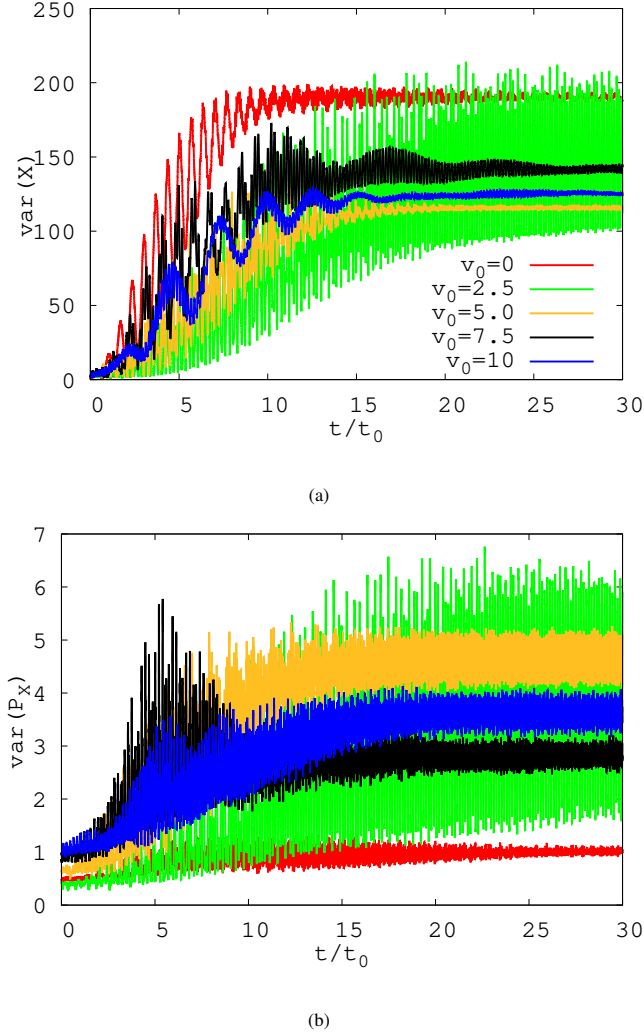


Figure 3: Plot of the many-particle position [panel (a)] and momentum variances [panel (b)] for various barrier heights V_0 . Here the results are obtained with $M = 4$ orbitals for $N = 100$ particles and interaction strength $\Lambda = 0.1$.

band plays the dominant role in the dynamics. Therefore, next, we examine the degree of fragmentation of the CBJJ when the second band (in addition to the lowest band) also plays a significant role in the dynamics. We present our results for different V_0 in Fig. 4. The panels in the left column show $\frac{n_i}{N}$ for the first two orbitals while those on the right column exhibit the same for the third and fourth orbitals.

For the symmetric double well ($V_0 = 0$), we get back the usual two-fold fragmentation with the $\frac{n_1}{N} \sim 60\%$ and $\frac{n_2}{N} \sim 40\%$ for all N keeping Λ fixed at 0.1. Although there are no macroscopic occupations in the higher orbitals for BJJ, we still observe the depletion of the same order in the third ($\frac{n_3}{N} \sim 10^{-3}$) and fourth ($\frac{n_4}{N} \sim 10^{-4}$) orbitals for all N .

For a finite V_0 , the system is now four-fold fragmented. However, we still find that over time $\frac{n_i}{N}$ for all four orbitals reaches a fixed value for various N corresponding to the same Λ for all V_0 studied here. However, as discussed above, the final values of $\frac{n_i}{N}$ change with an increase in V_0 and the particles of the system

become more evenly distributed among the four orbitals with reduced occupations in higher orbitals and increased occupations in lower orbitals. Therefore, even though the details of fragmentation vary for various trap geometry, the systems exhibit the universality of fragmentation for all four orbitals with respect to N corresponding to a fixed $\Lambda = 0.1$ irrespective of the value of V_0 . However, we have noticed that the pace of appearance of the universality of fragmentation depends on V_0 . As we switch on the internal barrier V_0 , for a small value of V_0 it takes longer to observe the universality of fragmentation than the symmetric double well ($V_0 = 0$). Then, as V_0 is increased, the universality appears faster. Furthermore, for a fixed value of V_0 , the system fragments later for larger N . This is expected as the many-body effects are reduced with increasing N keeping Λ fixed.

In our earlier study [30], we demonstrated that the universality of fragmentation is preserved in asymmetric BJJ. So, our present study in combination with the earlier findings indicates that the universality of fragmentation with respect to N is neither limited to systems where only two orbitals play a dominant role nor is susceptible to the geometry of the double well potential. Thus it is indeed a robust many-body effect.

4. Summary and conclusion

In this work, we reviewed the many-body tunnelling dynamics of an interacting Bose gas in a composite double well. The composite double well is formed by merging two deformed harmonic wells which have a hump at their centre. We examined the dynamics through the time evolution of survival probability, fragmentation, and many-particle variances. While survival probability may be studied at the mean-field level, fragmentation and many-particle variances are of purely many-body nature.

We found irregularity in the density oscillations for very small hump and then, two distinct oscillations for bigger hump. While the fast high-frequency oscillation is due to the tunnelling through the hump within the same well, the low-frequency tunnelling is due to the tunnelling between the two wells. Evidently, we need more than two orbitals to accurately describe such complicated many-body tunnelling. We observed (see appendix) that at least four orbitals are required for the accurate description of the many-body dynamics of the system contrary to the standard BJJ dynamics where two orbitals are sufficient.

The correlation between the damping of the density oscillation and the growth of fragmentation is already well-established. We observed that the same correlations still exist even for composite BJJ. However, the degree of fragmentation as well as the growth of the fragmentation significantly differ in the two cases. While the BJJ becomes two-fold fragmented, CBJJ is four-fold fragmented. On the other hand, the growth of fragmentation becomes slower in CBJJ except for very high hump V_0 . Accordingly, damping of density oscillations becomes slower in CBJJ. Furthermore, the occupations of different orbitals $\frac{n_i}{N}$ clearly show the more prominent participation of the third and fourth orbitals in the case of CBJJ. All

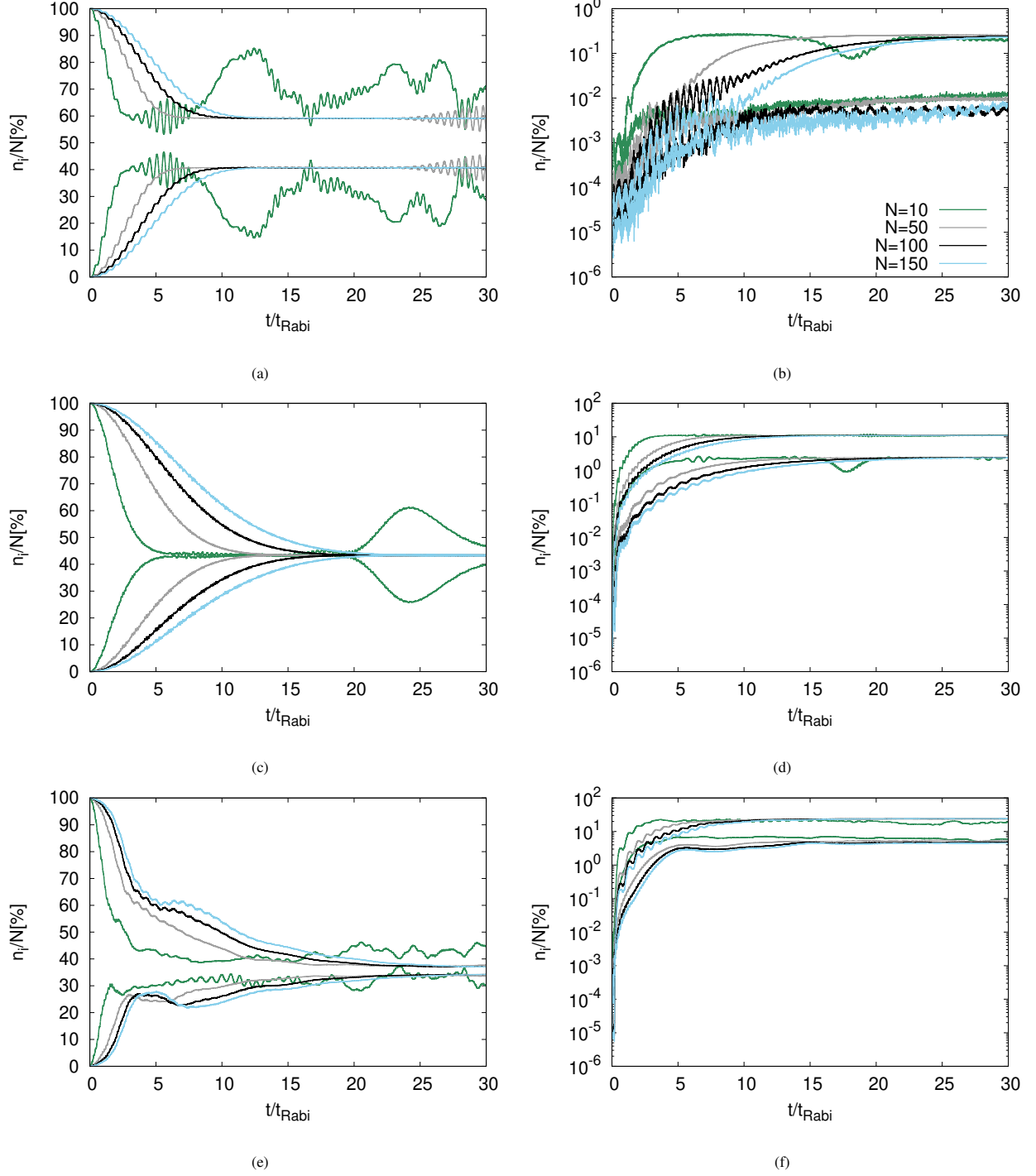


Figure 4: Universality of fragmentation in a symmetric double well (i.e. $V_0 = 0$) [panel (a) & panel (b)] and composite double well with $V_0 = 5$ [panel (c) & panel (d)], and $V_0 = 7.5$ [panel (e) & panel (f)]. In each row, the left panels show the occupations for the first two orbitals while the right panels show the occupation for the third and fourth orbitals. Since the occupations in higher orbitals are small, these are shown in the log scale. Colour codes are explained in panel (b). Results shown here are obtained with $M = 4$ for interaction strength $\Lambda = 0.1$.

these observations are further strengthened by the study of the many-particle position and momentum variances which exhibit higher fluctuations but slower growth.

Another interesting finding of this study is that the universality of the fragmentation with respect to the occupation in an orbital corresponding to a fixed interaction strength Λ is not

limited to systems where only two orbitals play dominant roles. Furthermore, not only universality is observed for orbitals with macroscopic occupations but even orbitals with microscopic occupations also have the same order of occupations with respect to different N but with a fixed Λ . And these features are observed for all V_0 which reaffirms that the universality of frag-

mentation is a global many-body phenomenon.

Thus we see that depending on the systems, the role of a different number of orbitals in the dynamics becomes dominant. Therefore, it is absolutely necessary to have a many-body method capable of taking into account all relevant orbitals for an accurate description of the complex many-body dynamics. The MCTDHB method is an important and promising many-body technique in this direction. The present work can inspire us to investigate the tunnelling dynamics of even more intriguing ground states of bosonic and fermionic ensembles.

Appendix A. The multi-configurational time-dependent Hartree method for bosons (MCTDHB)

Below we briefly describe the basic idea behind the method. In MCTDHB, the ansatz for solving Eq. (4) is obtained by the superposition of all possible $\binom{N+M-1}{N}$ configurations, obtained by distributing N bosons in M time-dependent single-particle states $\phi_k(x, t)$, which we call orbitals, i.e.,

$$|\Psi(t)\rangle = \sum_{\vec{n}} C_{\vec{n}}(t) |\vec{n}; t\rangle, \quad (\text{A.1})$$

where the occupations $\vec{n} = (n_1, n_2, \dots, n_M)$ preserve the total number of bosons N . For an exact theory, M should be infinitely large. However, for numerical computations, one has to truncate the series at a finite M . In actual calculations, we keep on increasing M until we reach the convergence with respect to M and thereby we obtain a numerically-exact result. In the context of bosons in a double well, the latter implies that the MCTDHB theory effectively takes all required bands into account. Here we would like to point out that for $M = 1$, the ansatz Eq. (A.1) gives back the ansatz for the Gross Pitaevskii theory [53]. Therefore, solving for the time-dependent wavefunction $\Psi(t)$ boils down to the determination of the time-dependent coefficients $\{C_{\vec{n}}(t)\}$ and the time-dependent orbitals $\{\phi_k(x, t)\}$. Employing the usual Lagrangian formulation of the time-dependent variational principle [54, 55] subject to the orthonormality between the orbitals, the working equations of the MCTDHB are obtained as follows

$$\begin{aligned} i|\dot{\phi}_j\rangle &= \hat{\mathbf{P}} \left[\hat{h} |\phi_j\rangle + \sum_{k,s,q,l=1}^M \{\rho(t)\}_{jk}^{-1} \rho_{ksql} \hat{W}_{sl} |\phi_q\rangle \right]; \\ \hat{\mathbf{P}} &= 1 - \sum_{j'=1}^M |\phi_{j'}\rangle \langle \phi_{j'}| \\ \mathbf{H}(t)\mathbf{C}(t) &= i \frac{\partial \mathbf{C}(t)}{\partial t}. \end{aligned} \quad (\text{A.2})$$

Here, $\rho(t)$ is the reduced one-body density matrix [see Eq. (A.3) below], ρ_{ksql} are the elements of the two-body reduced density matrix [see Eq. (A.4) below], and $\mathbf{H}(t)$ is the Hamiltonian matrix with the elements $H_{\vec{n}\vec{n}'}(t) = \langle \vec{n}; t | \hat{H} | \vec{n}'; t \rangle$. The one-body reduced density matrix used in Eq. (A.2) $\rho^{(1)}(x_1|x'_1; t)$ can be

defined through the normalized many-body wavefunction $\Psi(t)$ as

$$\begin{aligned} \rho^{(1)}(x_1|x'_1; t) &= \\ N \int dx_2 \dots dx_N \Psi^*(x'_1, x_2, \dots, x_N; t) \Psi(x_1, x_2, \dots, x_N; t) \\ &= \sum_{j=1}^M n_j(t) \phi_j^{*NO}(x'_1, t) \phi_j^{NO}(x_1, t). \end{aligned} \quad (\text{A.3})$$

Here, the time-dependent eigenfunctions $\phi_j^{NO}(x_1, t)$ of $\rho^{(1)}(x_1|x'_1; t)$ are the natural orbitals and $n_j(t)$ the time-dependent eigenvalues of $\rho^{(1)}(x_1|x'_1; t)$ are the natural occupation numbers. The diagonal of the $\rho^{(1)}(x_1|x'_1; t)$ gives the density of the system $\rho(x; t) \equiv \rho^{(1)}(x|x' = x; t)$.

Similarly, the two-body density can be calculated as

$$\begin{aligned} \rho^{(2)}(x_1, x_2|x'_1, x'_2; t) &= \\ N(N-1) \int dx_3 \dots dx_N \Psi^*(x'_1, x'_2, x_3, \dots, x_N; t) \\ &\quad \times \Psi(x_1, x_2, x_3, \dots, x_N; t). \end{aligned} \quad (\text{A.4})$$

Therefore, the matrix elements of the two-body reduced density matrix are given by $\rho_{ksql} = \langle \Psi | b_k^\dagger b_s^\dagger b_q b_l | \Psi \rangle$ where b_k and b_k^\dagger are the bosonic annihilation and creation operators, respectively.

Appendix B. Numerical implementation of MCTDHB

A parallel version of MCTDHB has been implemented using a novel mapping technique [56, 57]. We mention that by propagating in imaginary time the MCTDHB equations also allow one to determine the ground and excited state of interacting many-boson systems, see [58, 39]. In our present work, we have performed all computations with $M = 4$ time-adaptive orbitals. By repeating our computations with $M = 6, 8, 10$, and 12 orbitals the results have been verified and found to be highly accurate for the quantities and propagation times considered here.

In our numerical calculations, the many-body Hamiltonian is represented by 256 exponential discrete-variable-representation (DVR) grid points (using a Fast Fourier transformation routine) in a box size $[-10, 10]$. We obtain the initial state for the time propagation, the many-body ground state of the BEC by propagating the MCTDHB equations of motion [Eq. (A.2)] in imaginary time [58, 39]. For our numerical computations, we use the numerical implementation in [56, 57]. We keep on repeating the computation with increasing M until convergence is reached and thereby obtain the numerically accurate results.

Appendix C. Numerical convergence

As explained above, in actual calculation Eq. (A.1) is truncated at a finite M which is just sufficient for numerical convergence and thereby provides a numerically accurate description of the many-body dynamics. Here we have truncated Eq. (A.1) at $M = 4$. Therefore, now we demonstrate that $M = 4$ is enough for achieving a good degree of numerical convergence of our

results with respect to M . Here, we will explicitly show the numerical convergence of the dynamical quantities for a system of $N = 10$ only. Since in the limit $N \rightarrow \infty$, keeping Λ fixed, the many-body effects diminish and the density per particle of the system converge to its corresponding mean-field values [59, 60, 61, 62], the convergence of the quantities improves for higher N values for a fixed Λ . Therefore, the accuracy of our actual results discussed above is better than the results shown in this section.

As demonstrated in previous studies [8, 9], $M = 2$ orbitals are enough for an accurate description of the time evolution of all the dynamical quantities viz. $p_L(t)$, $\frac{n_i}{N}$, $\frac{1}{N^2}\Delta_X^2$ and $\frac{1}{N^2}\Delta_{P_X}^2$ of the BJJ even with a long-range interaction. Since the initial state for CBJJ is the ground state of BEC in a symmetric double well (BJJ), $M = 2$ should be enough for an accurate description of the initial state for the dynamics of CBJJ. However, here we computed the initial states with $M = 4$ orbitals as for studying the dynamics we would need at least $M = 4$ orbitals for CBJJ. Therefore, at the onset of our study, we can rest assured about the convergence of our initial state with respect to M .

Appendix C.1. Convergence of dynamical quantities

Now, we will discuss the convergence of the dynamics with respect to the M . We characterized the dynamics of the systems by the time evolution of the survival probability, fragmentation, and the many-particle position and momentum variances. However, it is well demonstrated that achieving convergence for the many-particle position and momentum variances are more challenging. Therefore, the demonstration of convergences for the many-particle position and momentum variances should automatically demonstrate the convergence of the survival probability as well as the fragmentation. Still, we will explicitly show the convergence of occupation numbers in addition to the convergence of the many-particle position and momentum variances as the characteristics of the time evolution of the fragmentation are directly related to the features of the many-particle position and momentum variances. Moreover, demonstration of convergence for systems with a higher degree of fragmentation would automatically imply convergence for systems with a lower degree of fragmentation as the many-body effects are diminished with the decrease in the occupations in higher orbitals. Therefore, demonstration of convergence of various quantities for $V_0 = 10$ would automatically imply the convergence for other V_0 considered in this work for which the system is less fragmented. We will discuss the convergence of these quantities with respect to M for the time duration discussed in this work.

Appendix C.1.1. Convergence of fragmentation and depletion

We start with the demonstration of convergence of the occupation numbers of different orbitals for composite BJJ. Although the demonstration of convergence for $V_0 = 10$ is sufficient, we still explicitly show the convergence for $V_0 = 7.5$ in addition to $V_0 = 10$ since in section 3.2 we showed the universality of fragmentation for V_0 up to $V_0 = 7.5$.

First, we consider the first four orbitals which have macroscopic

occupations for CBJJ (though the third and fourth orbitals for BJJ still have microscopic occupations). In Fig. C.5 we plot $\frac{n_i}{N}[\%]$ for the first 4 orbitals for different $M \geq 4$ to exhibit the convergence of our results. We observe that the results for $M = 4$ and $M = 8$ essentially overlap with each other for both $V_0 = 7.5$ and $V_0 = 10$. Since the many-body results smoothly approach the mean-field limit as N increases, our results for $N = 100$ accurately demonstrate the development of fragmentation in the course of the out-of-equilibrium many-body dynamics. Further, in Fig. C.6, we explicitly show that the occupations for the higher orbitals for $V_0 = 10$ are microscopically small.

Appendix C.1.2. Convergence of many-particle position and momentum variances

Next, we present the convergence results for $\frac{1}{N^2}\Delta_X^2$ and $\frac{1}{N^2}\Delta_{P_X}^2$ [Fig C.7]. For both $M = 4$ and $M = 8$ orbitals, we observe the same qualitative feature that $\frac{1}{N^2}\Delta_X^2$ increases with the growth of fragmentation and then exhibits an irregular oscillation [Fig C.7(a)]. In conformity with our findings of the fragmentation, here also we find a good degree of overlap between the fluctuations of $\frac{1}{N^2}\Delta_X^2$ for $M = 4$ and $M = 8$. Similarly, we notice a very high degree of overlapping between $\frac{1}{N^2}\Delta_{P_X}^2$ for $M = 4$ and $M = 8$ [Fig C.7(b)]. However, the deviation between the $\frac{1}{N^2}\Delta_{P_X}^2$ for $M = 4$ and $M = 8$ is slightly higher than $\frac{1}{N^2}\Delta_X^2$. This is expected as achieving convergence for $\frac{1}{N^2}\Delta_{P_X}^2$ is more difficult.

As the convergence significantly improves with increasing N , we can safely assume that the main findings for the system size $N = 100$ accurately demonstrate the many-body features of the out-of-equilibrium dynamics of a fragmented system.

Acknowledgements

SKH acknowledges the support from the Department of Science and Technology (DST), India, through TARE Grant No.: TAR/2021/000136. Work performed in Haifa is supported by the Israel Science Foundation (grant number 1516/19). Computation time on the High-Performance Computing system Hive of the Faculty of Natural Sciences at the University of Haifa and at the High-Performance Computing Center Stuttgart (HLRS) is gratefully acknowledged.

References

- [1] D. Petrov, D. Gangardt, G. Shlyapnikov, Low-dimensional trapped gases, *Journal de Physique IV (Proceedings)* 116 (2004) 5–44. doi:10.1051/jp4:2004116001.
- [2] K. Henderson, C. Ryu, C. MacCormick, M. G. Boshier, Experimental demonstration of painting arbitrary and dynamic potentials for bose–einstein condensates, *New Journal of Physics* 11 (4) (2009) 043030. doi:10.1088/1367-2630/11/4/043030. URL <https://dx.doi.org/10.1088/1367-2630/11/4/043030>
- [3] J. Ye, D. W. Vernooy, H. J. Kimble, Trapping of single atoms in cavity qed, *Phys. Rev. Lett.* 83 (1999) 4987–4990. doi:10.1103/PhysRevLett.83.4987. URL <https://link.aps.org/doi/10.1103/PhysRevLett.83.4987>

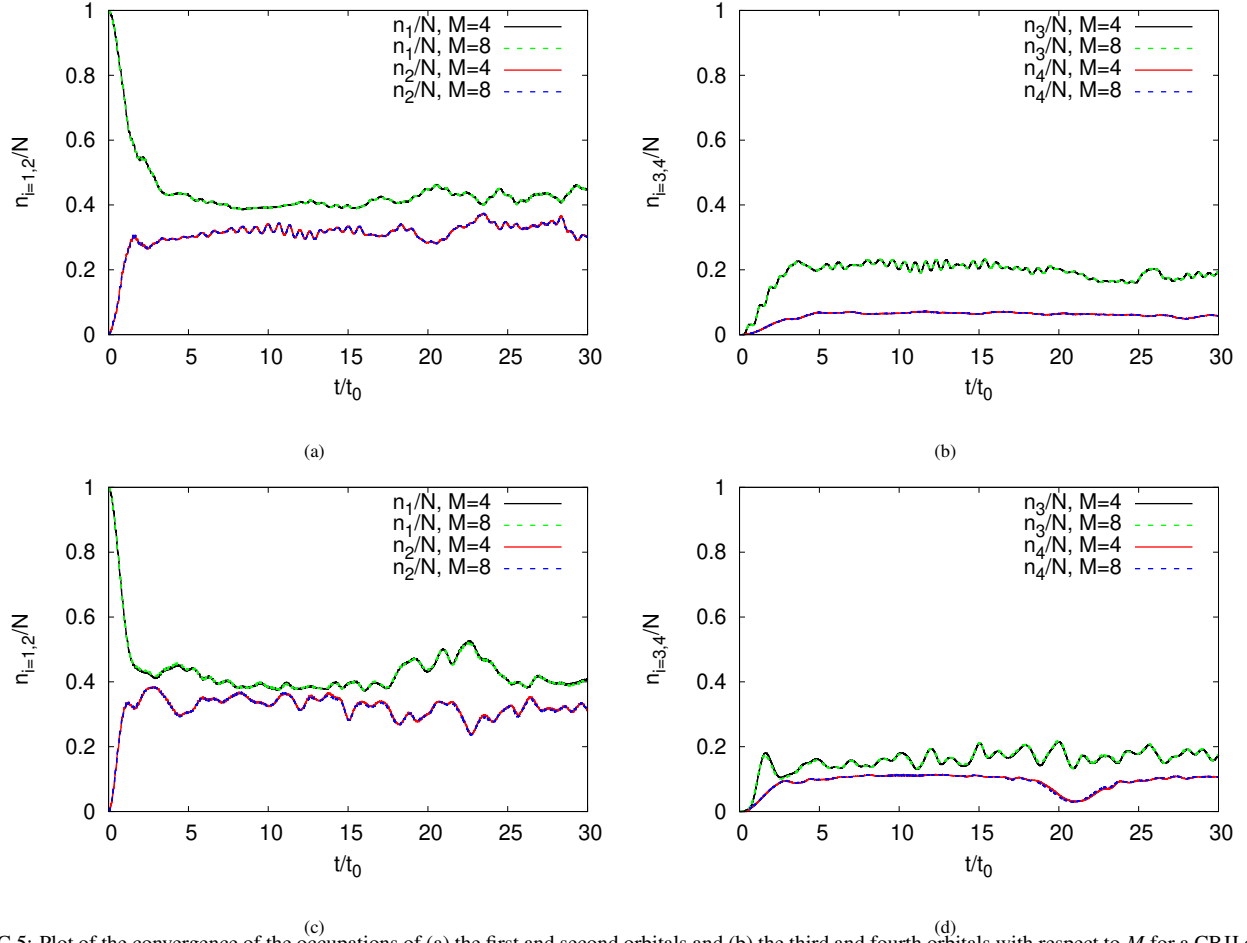


Figure C.5: Plot of the convergence of the occupations of (a) the first and second orbitals and (b) the third and fourth orbitals with respect to M for a CBJJ of barrier height $V_0 = 7.5$, $N = 10$, and $\Lambda = 0.1$. Convergence of occupation numbers for $V_0 = 10$, $N = 10$, and $\Lambda = 0.1$ are shown in panel (c) (first and second orbitals) and (d) (third and fourth orbitals) respectively.

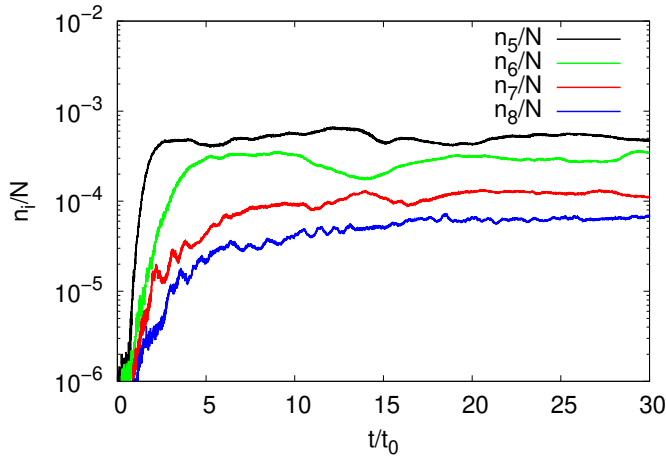


Figure C.6: Plot of occupations in higher $M > 4$ orbitals viz. $\frac{n_i}{N}$ ($i = 5, 6, 7$, and 8) for the composite BJJ with $V_0 = 10$.

- [4] C. E. Wieman, D. E. Pritchard, D. J. Wineland, Atom cooling, trapping, and quantum manipulation, *Rev. Mod. Phys.* 71 (1999) S253–S262. doi:10.1103/RevModPhys.71.S253. URL <https://link.aps.org/doi/10.1103/RevModPhys.71.S253>
- [5] P. Pinkse, T. Fischer, P. Maunz, G. Rempe, Trapping an atom with

single photons, *Nature* 404 (6776) (2000) 365–368. doi:10.1038/35006006.

URL <https://doi.org/10.1038/35006006>

- [6] A. Bhowmik, N. N. Dutta, S. Majumder, Tunable magic wavelengths for trapping with focused laguerre-gaussian beams, *Phys. Rev. A* 97 (2018) 022511. doi:10.1103/PhysRevA.97.022511. URL <https://link.aps.org/doi/10.1103/PhysRevA.97.022511>
- [7] C. Chin, R. Grimm, P. Julienne, E. Tiesinga, Feshbach resonances in ultracold gases, *Rev. Mod. Phys.* 82 (2010) 1225–1286. doi:10.1103/RevModPhys.82.1225. URL <https://link.aps.org/doi/10.1103/RevModPhys.82.1225>
- [8] K. Sakmann, A. I. Streltsov, O. E. Alon, L. S. Cederbaum, Exact quantum dynamics of a bosonic josephson junction, *Phys. Rev. Lett.* 103 (2009) 220601. doi:10.1103/PhysRevLett.103.220601. URL <https://link.aps.org/doi/10.1103/PhysRevLett.103.220601>
- [9] S. K. Haldar, O. E. Alon, Impact of the range of the interaction on the quantum dynamics of a bosonic josephson junction, *Chemical Physics* 509 (2018) 72–80, high-dimensional quantum dynamics (on the occasion of the 70th birthday of Hans-Dieter Meyer). doi:<https://doi.org/10.1016/j.chemphys.2018.01.017>. URL <https://www.sciencedirect.com/science/article/pii/S0301010417308881>
- [10] A. Bhowmik, S. K. Haldar, O. E. Alon, Impact of the transverse direction on the many-body tunneling dynamics in a two-dimensional bosonic josephson junction, *Scientific Reports* 10 (1) (dec 2020). doi:10.1038/s41598-020-78173-w.

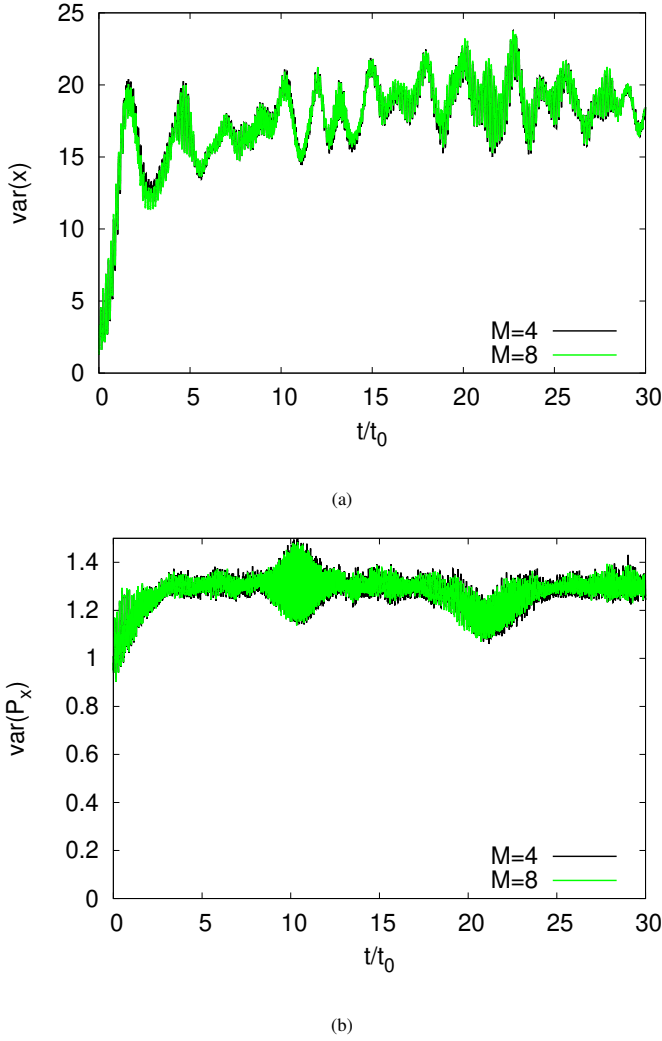


Figure C.7: Plot of the convergence of (a) many-particle position variance and (b) many-particle momentum variance with respect to M for a CBJJ of barrier height $V_0 = 10.0$, $N = 10$, and $\Lambda = 0.1$.

- URL <https://doi.org/10.1088/1367-2630/ab6eab>
<https://www.overleaf.com/project/637685d9a0c4d9f41a018b1f.1038%2F41598-020-78173-w>
- [11] B. Josephson, Possible new effects in superconductive tunnelling, *Physics Letters* 1 (7) (1962) 251–253. doi:[https://doi.org/10.1016/0031-9163\(62\)91369-0](https://doi.org/10.1016/0031-9163(62)91369-0). URL <https://www.sciencedirect.com/science/article/pii/0031916362913690>
- [12] K. Sakmann, A. I. Streltsov, O. E. Alon, L. S. Cederbaum, Universality of fragmentation in the schrödinger dynamics of bosonic josephson junctions, *Phys. Rev. A* 89 (2014) 023602. doi:10.1103/PhysRevA.89.023602. URL <https://link.aps.org/doi/10.1103/PhysRevA.89.023602>
- [13] F. Theel, K. Keiler, S. I. Mistakidis, P. Schmelcher, Entanglement-assisted tunneling dynamics of impurities in a double well immersed in a bath of lattice trapped bosons, *New Journal of Physics* 22 (2) (2020) 023027. doi:10.1088/1367-2630/ab6eab. URL <https://dx.doi.org/10.1088/1367-2630/ab6eab>
- [14] J. Vargas, M. Nuske, R. Eichberger, C. Hippler, L. Mathey, A. Hemmerich, Orbital many-body dynamics of bosons in the second bloch band of an optical lattice, *Phys. Rev. Lett.* 126 (2021) 200402. doi:10.1103/PhysRevLett.126.200402. URL <https://link.aps.org/doi/10.1103/PhysRevLett.126.200402>
- [15] S. Levy, E. Lahoud, I. Shomroni, J. Steinhauer, The a.c. and d.c. josephson effect in a bose einstein condensate, *Nature* 449 (2007) 579–83. doi:10.1038/nature06186.
- [16] M. Albiez, R. Gati, J. Fölling, S. Hunsmann, M. Cristiani, M. K. Oberthaler, Direct observation of tunneling and nonlinear self-trapping in a single bosonic josephson junction, *Phys. Rev. Lett.* 95 (2005) 010402. doi:10.1103/PhysRevLett.95.010402. URL <https://link.aps.org/doi/10.1103/PhysRevLett.95.010402>
- [17] G. J. Milburn, J. Corney, E. M. Wright, D. F. Walls, Quantum dynamics of an atomic bose-einstein condensate in a double-well potential, *Phys. Rev. A* 55 (1997) 4318–4324. doi:10.1103/PhysRevA.55.4318. URL <https://link.aps.org/doi/10.1103/PhysRevA.55.4318>
- [18] T. Schumm, S. Hofferberth, L. M. Andersson, S. Wildermuth, S. Groth, I. Bar-Joseph, J. Schmiedmayer, P. Krüger, Matter-wave interferometry in a double well on an atom chip, *Nature Physics* 1 (1) (2005) 57–62. doi:10.1038/nphys125. URL <https://doi.org/10.1038%2Fnpphys125>
- [19] C. Orzel, A. K. Tuchman, M. L. Fenselau, M. Yasuda, M. A. Kasevich, Squeezed states in a bose-einstein condensate, *Science* 291 (5512) (2001) 2386–2389. arXiv:<https://www.science.org/doi/pdf/10.1126/science.1058149>, doi:10.1126/science.1058149. URL <https://www.science.org/doi/abs/10.1126/science.1058149>
- [20] Q. Wu, L. Mancino, M. Carlesso, M. A. Ciampini, L. Magrini, N. Kiesel, M. Paternostro, Nonequilibrium quantum thermodynamics of a particle trapped in a controllable time-varying potential, *PRX Quantum* 3 (2022) 010322. doi:10.1103/PRXQuantum.3.010322. URL <https://link.aps.org/doi/10.1103/PRXQuantum.3.010322>
- [21] A. Smerzi, S. Fantoni, S. Giovanazzi, S. R. Shenoy, Quantum coherent atomic tunneling between two trapped bose-einstein condensates, *Phys. Rev. Lett.* 79 (1997) 4950–4953. doi:10.1103/PhysRevLett.79.4950. URL <https://link.aps.org/doi/10.1103/PhysRevLett.79.4950>
- [22] R. Gati, M. K. Oberthaler, A bosonic josephson junction, *Journal of Physics B: Atomic, Molecular and Optical Physics* 40 (10) (2007) R61. doi:10.1088/0953-4075/40/10/R01. URL <https://dx.doi.org/10.1088/0953-4075/40/10/R01>
- [23] L. J. LeBlanc, A. B. Bardon, J. McKeever, M. H. T. Extavour, D. Jervis, J. H. Thywissen, F. Piazza, A. Smerzi, Dynamics of a tunable superfluid junction, *Phys. Rev. Lett.* 106 (2011) 025302. doi:10.1103/PhysRevLett.106.025302. URL <https://link.aps.org/doi/10.1103/PhysRevLett.106.025302>
- [24] J. Gillet, M. A. Garcia-March, T. Busch, F. Sols, Tunneling, self-trapping, and manipulation of higher modes of a bose-einstein condensate in a double well, *Phys. Rev. A* 89 (2014) 023614. doi:10.1103/PhysRevA.89.023614. URL <https://link.aps.org/doi/10.1103/PhysRevA.89.023614>
- [25] A. Burchianti, C. Fort, M. Modugno, Josephson plasma oscillations and the gross-pitaevskii equation: Bogoliubov approach versus two-mode model, *Phys. Rev. A* 95 (2017) 023627. doi:10.1103/PhysRevA.95.023627. URL <https://link.aps.org/doi/10.1103/PhysRevA.95.023627>
- [26] J. Hou, X.-W. Luo, K. Sun, T. Bersano, V. Gokhroo, S. Mossman, P. Engels, C. Zhang, Momentum-space josephson effects, *Phys. Rev. Lett.* 120 (2018) 120401. doi:10.1103/PhysRevLett.120.120401. URL <https://link.aps.org/doi/10.1103/PhysRevLett.120.120401>
- [27] K. Sakmann, A. I. Streltsov, O. E. Alon, L. S. Cederbaum, Quantum dynamics of attractive versus repulsive bosonic josephson junctions: Bose-hubbard and full-hamiltonian results, *Phys. Rev. A* 82 (2010) 013620. doi:10.1103/PhysRevA.82.013620. URL <https://link.aps.org/doi/10.1103/PhysRevA.82.013620>
- [28] M. Khezri, J. Dressel, A. N. Korotkov, Qubit measurement error from

- coupling with a detuned neighbor in circuit qed, *Phys. Rev. A* 92 (2015) 052306. doi:10.1103/PhysRevA.92.052306.
URL <https://link.aps.org/doi/10.1103/PhysRevA.92.052306>
- [29] A. Bhowmik, O. E. Alon, Interference of longitudinal and transversal fragmentations in the josephson dynamics of bose-einstein condensates (2022). doi:10.48550/ARXIV.2207.05513.
URL <https://arxiv.org/abs/2207.05513>
- [30] S. K. Haldar, O. E. Alon, Many-body quantum dynamics of an asymmetric bosonic josephson junction, *New Journal of Physics* 21 (10) (2019) 103037. doi:10.1088/1367-2630/ab4315.
URL <https://dx.doi.org/10.1088/1367-2630/ab4315>
- [31] A. Bhowmik, O. E. Alon, Longitudinal and transversal resonant tunneling of interacting bosons in a two-dimensional josephson junction, *Scientific Reports* 12 (1) (January 2022). doi:10.1038/s41598-021-04312-6.
URL <https://doi.org/10.1038/s41598-021-04312-6>
- [32] S. Klaiman, A. I. Streltsov, O. E. Alon, Uncertainty product of an out-of-equilibrium many-particle system, *Phys. Rev. A* 93 (2016) 023605. doi:10.1103/PhysRevA.93.023605.
URL <https://link.aps.org/doi/10.1103/PhysRevA.93.023605>
- [33] D. Mondal, S. Sinha, S. Ray, J. Kroha, S. Sinha, Classical route to ergodicity and scarring phenomena in a two-component bose-josephson junction, *Phys. Rev. A* 106 (2022) 043321. doi:10.1103/PhysRevA.106.043321.
URL <https://link.aps.org/doi/10.1103/PhysRevA.106.043321>
- [34] T. Zibold, E. Nicklas, C. Gross, M. K. Oberthaler, Classical bifurcation at the transition from rabi to josephson dynamics, *Phys. Rev. Lett.* 105 (2010) 204101. doi:10.1103/PhysRevLett.105.204101.
URL <https://link.aps.org/doi/10.1103/PhysRevLett.105.204101>
- [35] M. Abbarchi, A. Amo, V. G. Sala, D. D. Solnyshkov, H. Flayac, L. Ferrier, I. Sagnes, E. Galopin, A. Lemaître, G. Malpuech, J. Bloch, Macroscopic quantum self-trapping and josephson oscillations of exciton polaritons, *Nature Physics* 9 (5) (2013) 275–279. doi:10.1038/nphys2609.
URL <https://doi.org/10.1038/nphys2609>
- [36] G. Valtolina, A. Burchianti, A. Amico, E. Neri, K. Xhani, J. A. Seman, A. Trombettoni, A. Smerzi, M. Zaccanti, M. Inguscio, G. Roati, Josephson effect in fermionic superfluids across the bec-bcs crossover, *Science* 350 (6267) (2015) 1505–1508. arXiv:https://www.science.org/doi/pdf/10.1126/science.aac9725, doi:10.1126/science.aac9725.
URL <https://www.science.org/doi/abs/10.1126/science.aac9725>
- [37] A. I. Streltsov, O. E. Alon, L. S. Cederbaum, Role of excited states in the splitting of a trapped interacting bose-einstein condensate by a time-dependent barrier, *Phys. Rev. Lett.* 99 (2007) 030402. doi:10.1103/PhysRevLett.99.030402.
URL <https://link.aps.org/doi/10.1103/PhysRevLett.99.030402>
- [38] O. E. Alon, A. I. Streltsov, L. S. Cederbaum, Multiconfigurational time-dependent hartree method for bosons: Many-body dynamics of bosonic systems, *Phys. Rev. A* 77 (2008) 033613. doi:10.1103/PhysRevA.77.033613.
URL <https://link.aps.org/doi/10.1103/PhysRevA.77.033613>
- [39] H. Kim, D. A. Huse, Heat and spin transport in a cold atomic fermi gas, *Phys. Rev. A* 86 (2012) 053607. doi:10.1103/PhysRevA.86.053607.
URL <https://link.aps.org/doi/10.1103/PhysRevA.86.053607>
- [40] M. Zhang, R. N. Lanning, Z. Xiao, J. P. Dowling, I. Novikova, E. E. Mikhailov, Spatial multimode structure of atom-generated squeezed light, *Phys. Rev. A* 93 (2016) 013853. doi:10.1103/PhysRevA.93.013853.
URL <https://link.aps.org/doi/10.1103/PhysRevA.93.013853>
- [41] J.-S. Bernier, C. Kollath, A. Georges, L. De Leo, F. Gerbier, C. Salomon, M. Köhl, Cooling fermionic atoms in optical lattices by shaping the confinement, *Phys. Rev. A* 79 (2009) 061601. doi:10.1103/PhysRevA.79.061601.
URL <https://link.aps.org/doi/10.1103/PhysRevA.79.061601>
- [42] J. Grond, T. Betz, U. Hohenester, N. J. Mauser, J. Schmiedmayer, T. Schumm, The shapiro effect in atomchip-based bosonic josephson junctions, *New Journal of Physics* 13 (6) (2011) 065026. doi:10.1088/1367-2630/13/6/065026.
URL <https://dx.doi.org/10.1088/1367-2630/13/6/065026>
- [43] A. U. J. Lode, C. Bruder, Dynamics of hubbard hamiltonians with the multiconfigurational time-dependent hartree method for indistinguishable particles, *Phys. Rev. A* 94 (2016) 013616. doi:10.1103/PhysRevA.94.013616.
URL <https://link.aps.org/doi/10.1103/PhysRevA.94.013616>
- [44] A. U. J. Lode, C. Bruder, Fragmented superradiance of a bose-einstein condensate in an optical cavity, *Phys. Rev. Lett.* 118 (2017) 013603. doi:10.1103/PhysRevLett.118.013603.
URL <https://link.aps.org/doi/10.1103/PhysRevLett.118.013603>
- [45] A. U. J. Lode, F. S. Diorico, R. Wu, P. Mollinari, L. Papariello, R. Lin, C. Lévêque, L. Exl, M. C. Tsatsos, R. Chitra, N. J. Mauser, Many-body physics in two-component bose-einstein condensates in a cavity: fragmented superradiance and polarization, *New Journal of Physics* 20 (5) (2018) 055006. doi:10.1088/1367-2630/aabc3a.
URL <https://dx.doi.org/10.1088/1367-2630/aabc3a>
- [46] B. Chatterjee, M. C. Tsatsos, A. U. J. Lode, Correlations of strongly interacting one-dimensional ultracold dipolar few-boson systems in optical lattices, *New Journal of Physics* 21 (3) (2019) 033030. doi:10.1088/1367-2630/aafa93.
URL <https://dx.doi.org/10.1088/1367-2630/aafa93>
- [47] J. G. Cosme, M. F. Andersen, J. Brand, Interaction blockade for bosons in an asymmetric double well, *Phys. Rev. A* 96 (2017) 013616. doi:10.1103/PhysRevA.96.013616.
URL <https://link.aps.org/doi/10.1103/PhysRevA.96.013616>
- [48] J. M. Schurer, A. Negretti, P. Schmelcher, Capture dynamics of ultracold atoms in the presence of an impurity ion, *New Journal of Physics* 17 (8) (2015) 083024. doi:10.1088/1367-2630/17/8/083024.
URL <https://dx.doi.org/10.1088/1367-2630/17/8/083024>
- [49] C. Lévêque, L. B. Madsen, Time-dependent restricted-active-space self-consistent-field theory for bosonic many-body systems, *New Journal of Physics* 19 (4) (2017) 043007. doi:10.1088/1367-2630/aa6319.
URL <https://dx.doi.org/10.1088/1367-2630/aa6319>
- [50] G. C. Katsimiga, S. I. Mistakidis, G. M. Koutentakis, P. G. Kevrekidis, P. Schmelcher, Many-body quantum dynamics in the decay of bent dark solitons of bose-einstein condensates, *New Journal of Physics* 19 (12) (2017) 123012. doi:10.1088/1367-2630/aa96f6.
URL <https://dx.doi.org/10.1088/1367-2630/aa96f6>
- [51] A. U. J. Lode, C. Lévêque, L. B. Madsen, A. I. Streltsov, O. E. Alon, Colloquium: Multiconfigurational time-dependent hartree approaches for indistinguishable particles, *Rev. Mod. Phys.* 92 (2020) 011001. doi:10.1103/RevModPhys.92.011001.
URL <https://link.aps.org/doi/10.1103/RevModPhys.92.011001>
- [52] S. Dutta, A. U. J. Lode, O. E. Alon, Fragmentation and correlations in a rotating bose-einstein condensate undergoing breakup, *Scientific Reports* 13 (1) (feb 2023). doi:10.1038/s41598-023-29516-w.
URL <https://doi.org/10.1038/s41598-023-29516-w>
- [53] F. Dalfovo, S. Giorgini, L. P. Pitaevskii, S. Stringari, Theory of bose-einstein condensation in trapped gases, *Rev. Mod. Phys.* 71 (1999) 463–512. doi:10.1103/RevModPhys.71.463.
URL <https://link.aps.org/doi/10.1103/RevModPhys.71.463>
- [54] P. Kramer, M. Saraceno, Geometry of the Time-Dependent Variational Principle in Quantum Mechanics, Vol. 140, Springer Berlin, 2007, pp. 112–121. doi:10.1007/3-540-10271-X_317.
- [55] H.-J. Kull, D. Pfirsich, Generalized variational principle for the time-dependent hartree-fock equations for a slater determinant, *Phys. Rev. E* 61 (2000) 5940–5947. doi:10.1103/PhysRevE.61.5940.
URL <https://link.aps.org/doi/10.1103/PhysRevE.61.5940>
- [56] A. I. Streltsov, O. I. Streltsova, Mctdhlb-lab: version 1.5 (2015).
URL <http://www.mctdhlb.com>
- [57] A. I. Streltsov, L. S. Cederbaum, O. E. Alon, K. Sakmann, A. U. J. Lode, J. Grond, O. I. Streltsova, S. Klaiman, R. Beinke, The multiconfigura-

- tional time-dependent hartree for bosons package, version 3.x, heidelberg/kassel (2006-present).
URL <http://mctdhub.org>
- [58] A. I. Streltsov, O. E. Alon, L. S. Cederbaum, General variational many-body theory with complete self-consistency for trapped bosonic systems, *Phys. Rev. A* 73 (2006) 063626. doi:10.1103/PhysRevA.73.063626.
URL <https://link.aps.org/doi/10.1103/PhysRevA.73.063626>
 - [59] E. H. Lieb, R. Seiringer, J. Yngvason, Bosons in a trap: A rigorous derivation of the gross-pitaevskii energy functional, *Phys. Rev. A* 61 (2000) 043602. doi:10.1103/PhysRevA.61.043602.
URL <https://link.aps.org/doi/10.1103/PhysRevA.61.043602>
 - [60] E. H. Lieb, R. Seiringer, Proof of bose-einstein condensation for dilute trapped gases, *Phys. Rev. Lett.* 88 (2002) 170409. doi:10.1103/PhysRevLett.88.170409.
URL <https://link.aps.org/doi/10.1103/PhysRevLett.88.170409>
 - [61] L. Erdős, B. Schlein, H.-T. Yau, Rigorous derivation of the gross-pitaevskii equation, *Phys. Rev. Lett.* 98 (2007) 040404. doi:10.1103/PhysRevLett.98.040404.
URL <https://link.aps.org/doi/10.1103/PhysRevLett.98.040404>
 - [62] L. Erdős, B. Schlein, H.-T. Yau, Derivation of the cubic non-linear schrödinger equation from quantum dynamics of many-body systems, *Inventiones mathematicae* 167 (3) (2006) 515–614. doi:10.1007/s00222-006-0022-1.
URL <https://doi.org/10.1007/s00222-006-0022-1>